RSC Advances

PAPER

View Article Online
View Journal | View Issue

Cite this: *RSC Adv.*, 2021, **11**, 37708

Novel mesoporous Ag@SiO_2 nanospheres as a heterogeneous catalyst with superior catalytic performance for hydrogenation of aromatic nitro compounds†

Wenyan Li, Xinying Lin, Jing Long, Bo Zheng, Zhaorui Pan, Leiming Lang* and Guangxiang Liu*

Received 12th September 2021
Accepted 16th November 2021

DOI: 10.1039/d1ra06853a

rsc.li/rsc-advances

Mesoporous core–shell structure Ag@SiO_2 nanospheres are constructed to prevent Ag nanoparticles from aggregation during the hydrogenation reaction. The prepared catalyst shows superior catalytic performance for hydrogenation of nitro compounds with 100% conversion and selectivity without any by-products, which also indicates good recycling performance for several times use.

Introduction

In recent years, selective hydrogenation reaction of aromatic nitro compounds has been an active area in chemistry because aromatic amino compounds are important industrial intermediates for pharmaceuticals, organic synthesis, agrochemicals, dyestuffs, urethanes and other important fine chemicals.[1–5] Although various commercial catalysts have been developed, the selective reduction of the nitro group from reducible functional groups needs stoichiometric reducing agents, such as iron, zinc, tin, or metal sulfide, which cause severe environmental problems and generate by-products.[6–12] Supported noble metal catalysts such as Pd/SiO_2,[13] Pt/C,[14,15] Au (Pd, Pt)/$Fe(OH)_x$,[16] Au/TiO_2,[17–20] Ni–Au[21] and Pt-rGO@mSiO_2 [22] have good catalytic performance, but the noble metal is quite rare and expensive. Silver-loaded catalysts have attracted scientists' attention and several works have been reported.[23–27] But, as comparison with gold catalysts, the study on catalytic hydrogenation of silver nanoparticles is relatively rare despite its' excellent catalytic performance. We are interested in the study on Ag nanocatalysis because it is a promise and undeveloped area. As we and other groups reported,[23–28] the high activity and selectivity for hydrogenation of the aromatic nitro compounds on the silver-loaded heterogeneous catalyst have been achieved, such as chemoselective hydrogenation of chloronitrobenzenes on Ag/Y_2O_3 nanobelt catalyst[26] and Ag/C_{60} catalyst[27] to corresponding chloroanilines without any hydrodehalogenation.

But we found that Ag nanoparticles (NPs) are easy to grow up. In order to prevent Ag NPs from growth, we have constructed Ag/Y_2O_3 nanobelts,[26] in which Ag NPs are partially embedded in Y_2O_3 nanobelts to stop Ag NPs from aggregation, but it failed. Then functionalized C_{60} supports were synthesized to fix Ag NPs,[27] it also failed to block the aggregation of Ag NPs. Finally, we constructed an Ag NPs@mesoporous SiO_2 core–shell nanostructure to solve this problem. The mesoporous shells benefit for the catalytic reaction because it permits molecules or ions pass through the pore freely and also prevents Ag NPs from aggregation. Although, up to now, several works about the preparation of core–shell nanostructures have been reported,[29–34] few of them investigate the hydrogenation reaction for core–shell structure sliver catalysts. Here, novel Ag@mesoporous silica spheres (A-MSS) catalyst was prepared and exhibited excellent catalytic performance for exclusive hydrogenation of nitro-group without any accumulation of hydroxylamine intermediates and formation of by-products.

Results and discussion

The core–shell structured A-MSS catalyst was prepared as follows (Scheme 1): Ag NPs were synthesized first by reducing

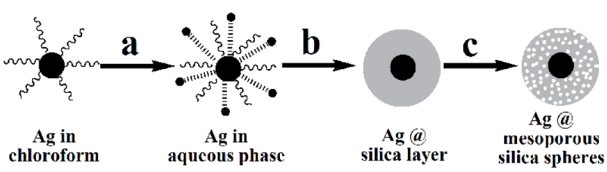

Scheme 1 Synthetic process of Ag@mesoporous silica spheres (A-MSS). (a) The transferation of Ag NPs from chloroform to aqueous phase using CTAB as phase transfer agent (▪▪▪▪). (b) The formation process of silica sol–gel on the surface of the Ag NPs in aqueous phase. (c) The formation of A-MSS by extraction using acetone at 70 °C.

Excellent Science and Technology Innovation Group of Jiangsu Province, Nanjing Xiaozhuang University, Nanjing 211171, China. E-mail: langleiming@njxzc.edu.cn; njuliugx@126.com

† Electronic supplementary information (ESI) available: Experimental section, EDS of A-MSS, Tables S1 and S2 of different catalysts catalytic activity and recycle performance. See DOI: 10.1039/d1ra06853a

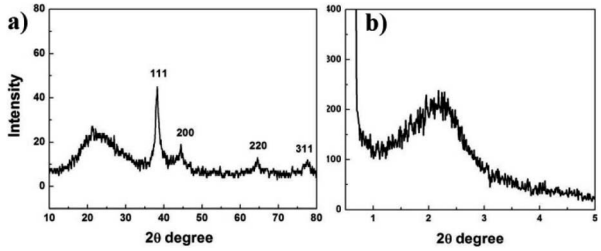

Fig. 1 (a) Wide-angle and (b) small-angle X-ray diffraction (XRD) patterns of A-MSS.

$AgNO_3$ in nonaqueous system, which dispersed in chloroform under the assistant of oleic acid and octadecylamine. Then, Ag NPs were transferred to aqueous phase from chloroform using CTAB as a phase transfer agent (also acted as a making hole-agent for the formation of the mesoporous silica). Finally, CTAB was removed by extraction using acetone.

Fig. 1a is the wide-angle XRD pattern of A-MSS at the 2θ degree range from 10° to 80°. A broad peak at 20–30° (2θ) corresponds to the amorphous SiO_2 and others are good agreement with the standard XRD pattern of f.c.c Ag (JCPDS card No. 04-0783). The broad reflection peak in small-angle XRD pattern of A-MSS (Fig. 1b) indicates the presence of a mesoporous structure without the long-range ordering.

TEM and HRTEM images in Fig. 2 provided an insight into the microstructure of product. TEM image in Fig. 2a shows that synthesized Ag NPs have very uniform size distribution with average diameter 7 nm. HRTEM image (Fig. 2b) shows interplanar crystal spacing of 0.245 nm attributed to the (111) lattice plane of fcc Ag NPs. The TEM image of A-MSS (Fig. 2c) reveals Ag NPs are wrapped by mesoporous silica. The scanning electron microscopy (SEM) image in Fig. 2d shows the quite uniform size with about 50 nm diameter, which is agreement with the results of Fig. 2c. The energy dispersive spectrum (EDS) in Fig. S1† shows that the catalyst contains 18.5 wt% of silver.

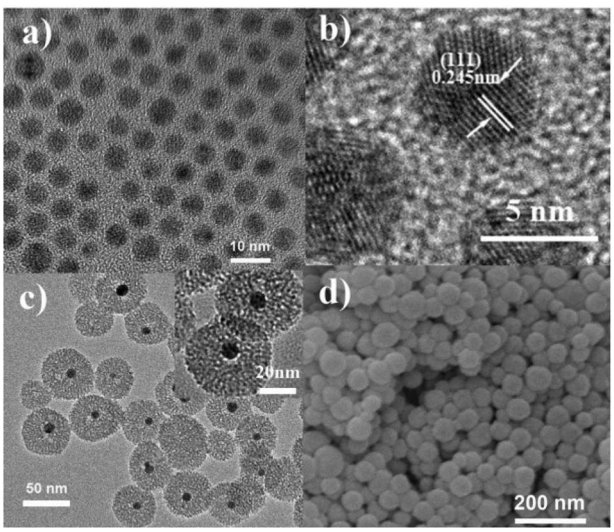

Fig. 2 TEM (a) and HRTEM (b) images of Ag NPs. TEM (c) and SEM (d) images of A-MSS (the enlarged A-MSS image in inset of c).

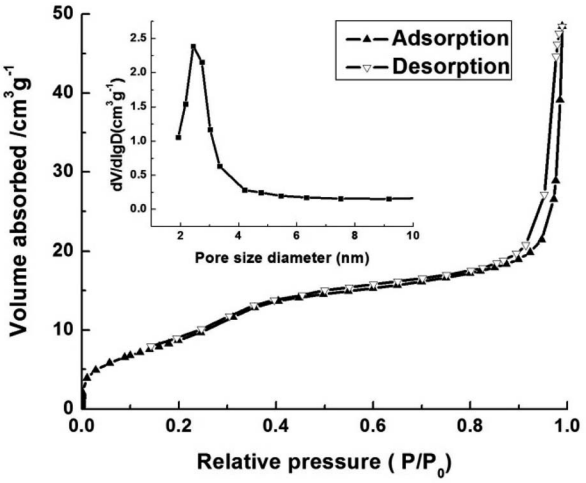

Fig. 3 Nitrogen adsorption/desorption isotherm and Barrett–Joyner–Halenda (BJH) pore size distribution plot (inset) of A-MSS.

To gain insights on the specific surface area and pore size distribution of the catalyst, Brunauer–Emmett–Teller (BET) N_2 adsorption–desorption measurement was conducted. As shown in Fig. 3, the A-MSS exhibits the typical type IV isotherm plot with an apparent hysteresis loop, indicative of a mesoporous microstructure. The BET analysis outputs a specific surface area value of ~742 $m^2 g^{-1}$. Meanwhile, the pore size distribution plot presents a sharp peak at ~2.2 nm, which demonstrates their mesoporous characteristics. The pore size calculated by the BJH (Barrett–Joyner–Halenda) method is about 2.5 nm, which corresponds to the result in the inset of Fig. 3.

To demonstrate the prepared A-MSS have high catalytic activity for hydrogenation reactions, we investigated this reaction system in details. Different reaction times and temperatures were screened (Table 1, entries 1–4) and it was found that the optimum reaction condition is 3 hours and 120 °C. The conversion and selectivity of the A-MSS were up to 100%, which will not need to prolong the reaction time or increase the reaction temperature. The solvent has a remarkable influence on the reaction. Water is not suitable for the reaction with a low conversion of 51.2% (Table 1, entry 5).

Table 1 Control experiments for hydrogenation of nitrobenzene to aniline on A-MSS[a]

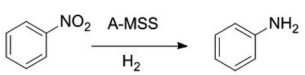

Entry	T (°C)	Time (h)	Conversion (%)	Selectivity (%)
1	100	2	25.2	100
2	120	2	78.5	100
3	120	2.5	85.6	100
4	120	3	100	100
5[b]	120	3	51.2	100

[a] Reaction conditions: 0.05 g catalyst, 0.5 g substrate and 30 mL ethanol, H_2 pressure 2.0 MPa. [b] The same conditions as a except 30 mL H_2O

Table 2 Hydrogenation of unsaturated substrates over A-MSS[a]

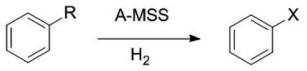

			Conversion (%)		Selectivity (%)	
Entry	R	X	120 (°C)	140 (°C)	120 (°C)	140 (°C)
1	$-NO_2$	$-NH_2$	100	100	100	100
2	$-CHCH_2$	$-CH_2CH_3$	0	16.8	0	100
3	–CHO	$-CH_2OH$	0	13.5	0	42.6[b]
4	$-COCH_3$	$-CH(OH)CH_3$	0	6.7	0	100
5	–CN	—	0	0	—	—
6	$-CH_2CN$	—	0	0	—	—
7	$-CONH_2$	—	0	0	—	—
8	$-NHCOCH_3$	—	0	0	—	—

[a] Reaction conditions: 0.05 g catalyst, 0.5 g substrate and 30 mL ethanol, H_2 pressure 3.0 MPa, and reaction time 3 h. [b] The only by-product is 2-hydroxypropiophenone.

Under the optimum reaction conditions the catalytic activity of A-MSS for the unsaturated substrates was investigated and the results were summarized in Table 2, which showed that A-MSS catalyzed the hydrogenation of nitrobenzene to aniline with 100% conversion and selectivity (Table 2, entry 1). Otherwise, A-MSS showed no or very low activity for the hydrogenation of styrene, benzaldehyde, acetophenone, benzonitrile, phenylacetonitrile, benzamide and acetanilide under the same condition (Table 2, entries 2–8). It is not easy to disclose the exact reason of the different hydrogenation activity for A-MSS, which maybe attribute to the exclusive hydrogenation selectivity of the catalyst for nitro-groups of the nitrobenzene derivatives and the different bond strength in the different groups.

In order to further evaluate the catalytic activity of A-MSS, various nitrobenzene derivatives were used as the starting materials and the results were listed in Table 3. Among them, the nitrobenzene derivatives containing electron-donating groups, such as chloro-, hydroxy- and methyl- groups, gave the complete conversion and selectivity without corresponding by-product to be detected (Table 3, entries 1–10). In case of nitrobenzaldehyde, nitroacetophenone, nitroacetanilide and nitrobenzonitrile, the conversion has an obvious decrease under the same mild reaction conditions (entries 11–14), which indicates that the existence of electron withdraw-groups such as nitrile-, aldehyde- and acyl- groups decrease the reactivity of the nitro-groups. But excellent conversion and selectivity can be achieved under serious conditions such as higher temperature, larger amount of catalyst and longer reaction time (entries 11–14). The high isolated yield can be achieved for nitrobenzene derivatives containing electron-donating groups (Table 3, entries 1–10), while low yield for other substrates (entries 11–14), which attributes to the low conversion and the separation loss of products.

The reuse performance of A-MSS was also investigated, which demonstrated the conversion and selectivity of the catalyst reused for five times have no obvious change (Table S1†). For comparison, we also prepared free Ag NPs and Ag/SiO_2 NPs by $NaBH_4$ reduction, which demonstrated the A-MSS catalyst has better catalytic activity and recycle performance (Table S2†). The superior catalytic performance of A-MSS can be attributed to the stable porous structure with the large surface area, which not only contributes reaction molecules to pass through the pores freely, but also makes the single Ag NPs isolate from other particles and avoid aggregating.

Conclusions

In this work, the size uniform A-MSS catalyst with Ag core and mesoporous silica shell was synthesized successfully, which has the large surface area and fine pore structure. Hydrogenation reaction of nitrobenzene derivatives was adopted as model reaction to evaluate the catalytic performance of the prepared catalyst. The results show that the A-MSS catalyst has the superior catalytic performance of 100% conversion and selectivity for the hydrogenation of nitro compounds with electron-donating or electron withdraw-groups under different reaction conditions. The catalyst can be reused for several times without an obvious change, which shows good recycle performance. The excellent catalytic activity attributes to the special mesoporous core–shell structure. The approach of synthesis can also be applied to achieve other similar structure catalysts for the hydrogenation of aromatic nitro compounds. The A-MSS catalyst can also be expected to replace the expensive noble metal catalysts and have more wide applications.

Experimental section

Synthesis of Ag NPs

Ag NPs were prepared by the pyrolysis of $AgNO_3$ in nonaqueous system. In a typical sample, 0.25 g $AgNO_3$ was added to 100 mL flask containing 15 mL oleic acid and 10 mL octadecylamine, heated to 280 °C at the rate of 7 °C min^{-1} and kept at this temperature for 30 minutes under slowly stirring. The product was isolated and washed for several times with mixed solution of ethanol and *n*-heptane.

Table 3 Hydrogenation of substituted nitrobenzene over A-MSS[a]a

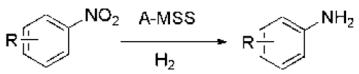

Entry	R	Product	Conversion (%)	Selectivity (%)	Isolated yield (%)
1	H		100	100	90
2	2-Cl		100	100	88
3	3-Cl	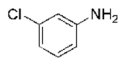	100	100	86
4	4-Cl	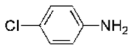	100	100	91
5	2-OH		100	100	87
6	3-OH	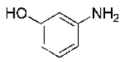	100	100	82
7	4-OH	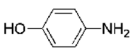	100	100	85
8	2-CH_3		100	100	90
9	3-CH_3	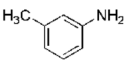	100	100	86
10	4-CH_3	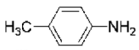	100	100	90
11	4-CHO	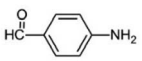	71 (100[b])	100	53
12	4-$COCH_3$	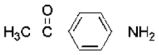	65 (100[b])	100	45
13	4-CN	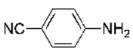	62 (93.5[b])	100	35
14	4-$CONH_2$	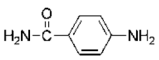	67 (100[a])	100	41

[a] Reaction conditions: 0.05 g catalyst, 0.5 g substrate and 30 mL ethanol, H_2 pressure 2.0 MPa; reaction temperature 120 °C; reaction time 3 h. [b] Reaction conditions: 0.1 g catalyst, 0.5 g substrate and 30 mL ethanol, H_2 pressure 3.0 MPa; reaction temperature 140 °C; reaction time 4 h.

Synthesis of core–shell structured Ag NPs@mesoporous silica spheres

The transparent solution of the Ag nanoparticles dispersed in 10 mL chloroform was added to 250 mL flask containing 50 mL of 0.06 M CTAB aqueous solution under vigorous mechanic stirring. After a moment, the chloroform was removed by heating the mixture at 70 °C, then centrifugated at 10 000 r.p.m. for 2 minutes in order to remove the large nanoparticles. The filtrate was mixed with 140 mL water and 40 mL ethanol, and then 2.5 mL of 0.2 M NaOH solution was added under stirring. Subsequently, 20 mL of 5% TEOS in ethanol was injected slowly. The product was precipitated by ethanol or acetone after four days, and isolated by centrifugating. Then the CTAB was removed by extraction using acetone at 70 °C. Finally, the sample was dried in vacuum at 50 °C for characterization.

Conflicts of interest

There are no conflicts to declare.

Acknowledgements

The authors are grateful for National Natural Science Foundation of China (No. 21671117).

Notes and references

1 J. Li, T. Zhao, T. Chen, Y. Liu, C. N. Ong and J. Xie, *Nanoscale*, 2015, **7**, 7502.
2 J. Gao, R. Ma, L. Feng, Y. Liu, R. Jackstell, R. V. Jagadeesh and M. Beller, *Angew. Chem.*, 2021, **133**, 18739.

3 L. Zhu, T. Zheng, J. Zheng, C. Yu, N. Zhang, Q. Zhou, W. Zhang and B. Chen, *CrystEngComm*, 2018, **20**, 113.
4 J. Song, Z. Huang, L. Pan, K. Li, X. Zhang, L. Wang and J. Zou, *Appl. Catal., B*, 2018, **227**, 386.
5 A.-M. Alexander and J. S. Hargreaves, *Chem. Soc. Rev.*, 2010, **39**, 4388.
6 J. Song, Z. Huang, L. Pan, K. Li, X. Zhang, L. Wang and J. Zou, *Appl. Catal., B*, 2018, **227**, 386.
7 P. Serna and A. Corma, *ACS Catal.*, 2015, **5**, 7114.
8 R. V. Jagadeesh, A. E. Surkus, H. Junge, M. M. Pohl, J. Radnik, J. Rabeah, H. Huan, V. Schunemann, A. Bruckner and M. Beller, *Science*, 2013, **342**, 1073.
9 A. Grirrane, A. Corma and H. Garcia, *Science*, 2008, **322**, 1661.
10 L. Zhu, T. Zheng, J. Zheng, C. Yu, N. Zhang, Q. Liao, Q. Shu and B. H. Chen, *CrystEngComm*, 2017, **19**, 3430.
11 P. Concepcion, A. Corma, J. Silvestre-Albero, V. Franco and J. Y. Chane-Ching, *J. Am. Chem. Soc.*, 2004, **126**, 5523.
12 A. Sepulveda-Escribano, F. Coloma and F. Rodriguez-peinoso, *J. Catal.*, 1998, **178**, 649.
13 A. J. Amali and R. K. Rana, *Chem. Commun.*, 2008, **35**, 4165.
14 F. Visentin, G. puxty, O. M. Kut and K. Hungerbuehler, *Ind. Eng. Chem. Res.*, 2006, **45**, 4544.
15 A. Corma, P. Sema, P. Conerpcion and J. J. Calvino, *J. Am. Chem. Soc.*, 2008, **130**, 8478.
16 L. Liu, B. Qiao, Z. Chen, J. Zhang and Y. Deng, *Chem. Commun.*, 2009, **6**, 653.
17 A. Corma and P. Serna, *Science*, 2006, **313**, 332.
18 A. Corma, P. Serna and H. Garcia, *J. Am. Chem. Soc.*, 2007, **129**, 6358.
19 A. Corma, P. ConcepciÓn and P. Serna, *Angew. Chem., Int. Ed.*, 2007, **46**, 7266.
20 M. Boronat, P. Concepción, A. Corma, S. González, F. Illas and P. Serna, *J. Am. Chem. Soc.*, 2007, **129**, 16230.
21 L. Lang, Z. Pan and J. Yan, *J. Alloys Compd.*, 2019, **792**, 286.
22 L. Shang, T. Bian, B. Zhang, D. Zhang, L. Z. Wu, C. H. Tung, Y. Yin and T. Zhang, *Angew. Chem., Int. Ed.*, 2014, **53**, 250.
23 M. Pashaei and E. Mehdipour, *Appl. Organomet. Chem.*, 2018, **32**, e4226.
24 M. Abbas, S. R. Toratia and C. Kim, *Nanoscale*, 2015, **7**, 12192.
25 J. Zheng, X. Duan, H. Lin, Z. Gu, H. Fang, J. Li and Y. Yuan, *Nanoscale*, 2016, **8**, 5959.
26 M. Han, X. Li, B. Li, N. Shi, K. Chen, J. Zhu and Z. Xu, *J. Phys. Chem. C*, 2008, **112**, 17893.
27 B. Li, H. Li and Z. Xu, *J. Phys. Chem. C*, 2009, **113**, 21526.
28 B. Li and Z. Xu, *J. Am. Chem. Soc.*, 2009, **131**, 16380.
29 M. Cai, Y. Li, Q. Liu, Z. Xue, H. Wang, Y. Fan, K. Zhu, Z. Ke, C. Su and G. Li, *Adv. Sci.*, 2019, **6**, 1802365.
30 R. Purbiaa and S. Paria, *Nanoscale*, 2015, **7**, 19789.
31 P. M. Arnal, M. Comotti and F. Schüth, *Angew. Chem., Int. Ed.*, 2006, **45**, 8224.
32 B. Banerjee, R. Singuru, S. K. Kundu, K. Dhanalaxmi, L. Bai, Y. Zhao, B. M. Reddy, A. Bhaumik and J. Mondal, *Catal. Sci. Technol.*, 2016, **6**, 5102.
33 L. Lang, Y. Shi, J. Wang, F. Wang and X. Xia, *ACS Appl. Mater. Interfaces*, 2015, **7**, 9098.
34 J. Y. Sun, Z. K. Wang, H. S. Lim, S. C. Ng, M. H. Kuok, T. T. Tran and X. Lu, *ACS Nano*, 2010, **4**, 7692.